Distributed On-Off Power Control for Amplify-and-Forward Relays with Orthogonal Space-Time Block Code

Mingjun Dai, Chi Wan Sung, and Yan Wang

***Abstract*—A single source-destination pair communicating via a layer of parallel relay nodes under quasi-static slow fading environment is investigated. One existing transmission protocol is considered, namely, the combination of the distributed version of the half symbol-rate complex constellation orthogonal space-time block codes (OSTBC) with adaptive amplify-and-forward (AAF) relaying strategy. We call this transmission protocol as distributed orthogonal space-time block coded adaptive amplify-and-forward (DOSTBC-AAF). To improve the performance of DOSTBC-AAF, a distributed on-off power control (OOPC) rule applied to the relays is analytically derived and is proved to achieve full diversity order. The outage performance of DOSTBC-AAF with and without power control is evaluated. Our simulation results show that DOSTBC-AAF with all relays transmitting at full power (FP) achieves no diversity gain, whereas DOSTBC-AAF with OOPC achieves full diversity order. Correspondingly, at high signal-to-noise ratio (SNR), the diversity-multiplexing tradeoff (DMT) achieved by DOSTBC-AAF (OOPC) is analytically derived and is numerically shown to outperform DOSTBC-AAF (FP) significantly.**

***Index Terms*—Orthogonal space-time block codes (OSTBC), amplify-and-forward (AF), parallel relay network, power control.**

I. Introduction

In a fading environment, multiple-antennas technique is effective to increase the capacity and reliability of a point-to-point multiple-input multiple-output (MIMO) wireless system [1]. If channel state information (CSI) of a communication link is available at both the transmitter (CSIT) and the receiver (CSIR) side, the transmitter and the receiver can adopt transmit beamforming and maximal ratio combining, respectively. This can co-phase the received signals from different paths, hence increasing the received signal-to-noise ratio (SNR). If only CSIR is assumed, space-time (ST) codes [2], [3] mimic transmit beamforming quite well though losing some power efficiency. As a result, ST codes are a good choice.

ST codes can be divided into two categories: space-time trellis code (STTC) [2] and space-time block codes (STBC), with the latter includes several variations, such as Khatri-Rao space-time (KRST) code [4], orthogonal STBC (OSTBC) [3], [5], and quasi-orthogonal STBC (QOSTBC) [6], [7]. Within ST codes family, the decoding complexity of STTC, KRST, and QOSTBC grows rapidly with the number of transmit antennas (TA) [8], [9], [10], [11], only OSTBC enjoys fast decoupled symbol-wise maximum-likelihood (ML) detection, whose complexity is linear with the number of TAs. The benefit of offering full diversity and decreased decoding complexity makes OSTBC attractive for low-complexity wireless networks. Normally, people pay attention to complex OSTBC with word "complex" meaning that the signal constellation is complex, since more dimensions are utilized compared to real codes. Within complex OSTBC designs, though there are high symbol-rate designs such as the 3/4 symbol-rate complex OSTBC [5], [12], which is dedicated to three and four antennas only, the half symbol-rate complex OSTBC [5] can be applied to arbitrary number of TAs [13], [14]. Besides, for large number of TAs, the half symbol-rate complex OSTBC approaches the theoretical maximal symbol-rate, $\lim_{m\to\infty} \frac{m+1}{2m} = \frac{1}{2}$ [15], where number of Tx antennas is $2m$ or $2m-1$.

Although multiple-antennas enjoys high received SNR, hence good reliability performance, the cost of deploying multiple antennas is quite high. Therefore, it is more practical to equip each terminal with single antenna. One solution to keep multiple-antennas' good property is to let a number of single-antenna nodes cooperatively act as a virtual antenna array [16]. Based on this intuition, parallel relay network, in which a source node and a destination node are connected by a number of parallel relay nodes, was proposed and investigated in [17] for the additive white Gaussian noise (AWGN) channel. The fading case assuming both CSIT and CSIR, is investigated in [18], [19]. For the fading case assuming CSIR only, similar to the MIMO case mentioned in the first pargraph, distributed version of OSTBC (DOSTBC) [20], which is cooperatively applied on the relay nodes by treating each relay node as an antenna, can achieve high diversity-multiplexing tradeoff (DMT) performance. As word "distributed" indicates, DOSTBC differs OSTBC in two folds: One is the existence of asynchronism between relay nodes for DOSTBC, and the other is the lack of information share between relay nodes for DOSTBC. For one-way communication, since the feedback channel can adjust each relay node's transmission time, we can assume synchronized DOSTBC, which works as a building block for investigation of asynchronized DOSTBC.

Beside DOSTBC which is cooperatively applied at the relay

Manuscript received July 16, 2010; revised January 3, 2011; accepted March 9, 2011. The associate editor coordinating the review of this paper and approving it for publication was L. Yang.

This work was partially supported by a grant from the University Grants Committee of the Hong Kong Special Administrative Region, China (Project No. AoE/E-02/08).

The authors are with the Department of Electronic Engineering, City University of Hong Kong, Kowloon, Hong Kong (e-mail: mingjudai2@student.cityu.edu.hk, albert.sung@cityu.edu.hk).

Digital Object Identifier 10.1109/TWC.2011.040511.101285

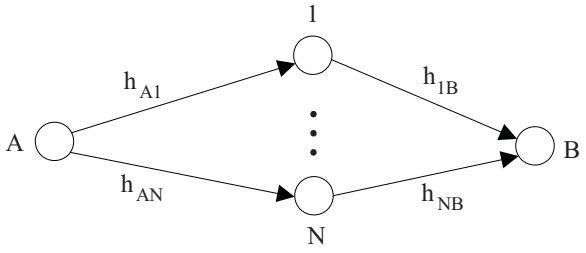

Fig. 1. The parallel relay network model.

nodes, at each relay node, there involves relaying techniques, including amplify-and-forward (AF) and decode-and-forward (DF), etc. AF can be divided into two categories: fixed-gain AF (FGAF), whose amplifying factor is fixed, and adaptive AF (AAF), whose amplifying factor depends on the instantaneous CSI of its input channel.

There are a lot of variations that combine DOSTBC with DF [21], with FGAF [22]-[26], and with AAF [27]. It is shown that DOSTBC combined with DF [21] and with FGAF [22]-[26] can achieve full diversity order in terms of the number of parallel relay nodes, respectively. However, DF suffers from high complexity, high energy consumption; FGAF may drive the transmit amplifier at the relay node into saturation, while the amplifying factor of AAF can be adjusted to avoid saturation. However, how to set the amplifying factor has yet to be specified. It is observed in Scheme 3 of [27] that letting all the relays always transmit with full power (FP) achieves diversity order no more than one. It is important to investigate whether DOSTBC combined with AAF can reap full diversity order.

In this paper, we apply both DOSTBC and AAF (DOSTBC-AAF) at the relay nodes. In particular, we combine the half symbol-rate complex DOSTBC with AAF and show that it can achieve full diversity by appropriate power control. If all the relay nodes always use FP, i.e., the amplifying factor of each relay node is set to be its maximum value, our simulation result shows that the achieved diversity order is one. To decrease the end-to-end outage probability, we analytically derive an on-off power control (OOPC) rule for DOSTBC-AAF. With this rule, we prove that DOSTBC-AAF (OOPC) can achieve full diversity. Besides, DOSTBC-AAF (OOPC) can be applied to arbitrary number of parallel relay nodes, and enjoys simple operation at the relay nodes and the destination node. The operation at the relay nodes is on-off AF and that at the destination node is decoupled symbol-wise ML decoding. We remark that this work is a non-trivial generalization of the power control rule in [28] to more than two parallel relay nodes.

II. System Model

We consider a single source communicating to a single destination in a network over a layer of $N > 2$ parallel relay nodes. There is no direct link from the source to the destination. As shown in Fig. 1, information source A has a single transmit antenna, and final destination B has a single receive antenna. The N relays are respectively denoted as relay $i \in \{1, 2, \ldots, N\} \triangleq \mathcal{N}$, each having a single antenna which can transmit and receive simultaneously. Note that the results obtained based on this full-duplex relay assumption can be directly applied to the half-duplex case. We consider the slow-fading scenario where the link gains are random but remain constant for a transmission block of $2P$ symbol times. Let h_{Ai} and h_{iB} be the link gains from source A to relay i and from relay i to destination B respectively, $i \in \mathcal{N}$. Define column vectors $\boldsymbol{h}_B \triangleq (h_{1B}, \ldots, h_{NB})$ and $\boldsymbol{h} \triangleq (h_{A1}, \ldots, h_{AN}, h_{1B}, \ldots, h_{NB})$. We assume that CSI of a communication link is available at its receiver but not at its transmitter, i.e., we assume CSIR only. More specifically, relay i knows h_{Ai}, and the destination node knows $\boldsymbol{h}$.

Let $X_i[m]$ denote the transmitted codeword from node i at time instant m, $i \in \{A\} \bigcup \mathcal{N}$, $Y_i[m]$ and $w_i[m]$ denote the received codeword and the thermal noise at node i at time instant m, $i \in \{B\} \bigcup \mathcal{N}$. Each channel's input-output relationship is represented by the following formulas:

$$Y_i[m] = h_{Ai} X_A[m] + w_i[m] \text{ for } i \in \mathcal{N}, \tag{1}$$

$$Y_B[m] = \sum_{i=1}^{N} h_{iB} X_i[m] + w_B[m], \tag{2}$$

subject to the power of $X_A[m]$, averaging over a transmission block of P symbols, is less than P_A, and that of $X_i[m]$, averaging over a transmission block of $2P$ symbols, is less than P_i for $i \in \mathcal{N}$. The reason why the constraints are imposed in this way will become clear after we describe how the half symbol-rate STBC is integrated into our transmission scheme in the next two sections. We further assume that $P_i \triangleq \kappa P_A$, $i \in \mathcal{N}$. Let $w_i[m], w_B[m] \sim \mathcal{CN}(0, \delta_w^2)$. Define $\Gamma \triangleq P_A/\delta_w^2$. The instantaneous received SNR at relay i is denoted by Γ_i, and is equal to $|h_{Ai}|^2\Gamma$. The instantaneous received SNR at destination B is denoted by $\Gamma_B(\boldsymbol{h})$, whose value depends on the transmission scheme. Correspondingly, we define $R_A(\boldsymbol{h})$ as the instantaneous end-to-end information rate from source A to destination B, and it is equal to $R_A(\boldsymbol{h}) = \log_2(1 + \Gamma_B(\boldsymbol{h}))$.

An outage event occurs if $R_A(\boldsymbol{h})$ falls below a certain threshold, R_{thd}. Outage probability is the probability of occurrence of an outage event, i.e., $p_{out} \triangleq \Pr\{R_A(\boldsymbol{h}) < R_{thd}\}$. The ϵ-outage rate R_ϵ for a certain scheme is defined as the value of R_{thd} such that $p_{out} = \epsilon$ holds. It is clearly a function of Γ. There is a one-to-one correspondence between $R_A(\boldsymbol{h})$ and $\Gamma_B(\boldsymbol{h})$. Therefore, the outage probability can also be obtained by comparing $\Gamma_B(\boldsymbol{h})$ with $\Gamma_{thd} \triangleq 2^{R_{thd}} - 1$. More specifically, we have $p_{out} = \Pr\{\Gamma_B(\boldsymbol{h}) < \Gamma_{thd}\}$.

Remark: Throughout this paper, we use superscript ^{T}, *, and † to denote the transpose, conjugate, and the conjugate transpose operation, respectively. We let superscript $^{(R)}$ and $^{(I)}$ denote the real part and imaginary part of a complex number/vector/matrix, respectively.

III. Generalized Orthogonal Designs

In this section, we present some terminologies in the theory of generalized orthogonal designs [5], and derive some new properties of a particular design, which will be used in the subsequent sections. We first introduce the following two notions defined in [5], [29]:

Definition 1: A generalized real orthogonal design (GROD) $\boldsymbol{G}$ of size N is a $P \times N$ matrix with entries $0, x_1, x_2, \ldots, x_K, -x_1, -x_2, \ldots, -x_K$, where $x_1, x_2, \ldots, x_K$ are indeterminates over the real field, satisfying $\boldsymbol{G}^T\boldsymbol{G} = (x_1^2 + x_2^2 + \cdots + x_K^2)\boldsymbol{I}_N$, where $\boldsymbol{I}_N$ is the $N \times N$ identity matrix. The symbol-rate of $\boldsymbol{G}$ is defined as K/P.

Definition 2: A generalized complex orthogonal design (GCOD) $\boldsymbol{G}_c$ of size N is a $P_c \times N$ matrix with entries 0, or $x_1, x_2, \ldots, x_K, -x_1, -x_2, \ldots, -x_K$, or their conjugates $x_1^*, x_2^*, \ldots, x_K^*, -x_1^*, -x_2^*, \ldots, -x_K^*$, or the products of the above ones with the imaginary unit j, where $x_1, x_2, \ldots, x_K$ are indeterminates over the complex field, satisfying $\boldsymbol{G}_c^\dagger\boldsymbol{G}_c = \gamma(|x_1|^2 + |x_2|^2 + \cdots + |x_K|^2)\boldsymbol{I}_N$, where γ is a constant. The symbol-rate of $\boldsymbol{G}_c$ is defined as K/P_c.

In this paper, we adopt the half symbol-rate GCOD constructed in [5], since it can be applied to arbitrary number of TAs/relay nodes. It is constructed by concatenating a GROD with its conjugate:

$$\boldsymbol{G}_c \triangleq \begin{bmatrix} \boldsymbol{G} \\ \boldsymbol{G}^* \end{bmatrix}, \tag{3}$$

where $\boldsymbol{G} \triangleq [g_{ji}]_{P\times N}$ is a GROD. How to construct $\boldsymbol{G}$ can be found in [5]. An example for $N = 3$ is given below:

$$\boldsymbol{G}_c^3 = \begin{bmatrix} x_1 & -x_2 & -x_3 & -x_4 & x_1^* & -x_2^* & -x_3^* & -x_4^* \\ x_2 & x_1 & x_4 & -x_3 & x_2^* & x_1^* & x_4^* & -x_3^* \\ x_3 & -x_4 & x_1 & x_2 & x_3^* & -x_4^* & x_1^* & x_2^* \end{bmatrix}^T. \tag{4}$$

The symbol-rate of $\boldsymbol{G}_c$ is $K/2P$ by definition and is equal to $1/2$ according to [5]. We then obtain $K = P$. In other words, the symbol-rate of $\boldsymbol{G}$ is equal to one. In the following, we will use P and K interchangeably. We index the upper half of $\boldsymbol{G}_c$ by $\mathcal{P}_{\text{real}} \triangleq \{1, 2, \ldots, P\}$, and the lower half by $\mathcal{P}_{\text{comp}} \triangleq \{P+1, P+2, \ldots, 2P\}$, with each index representing transmission time instant, since one row of $\boldsymbol{G}_c$ is transmitted by the antennas each time. The $2P$ transmissions compose a *transmission block*.

Lemma 1: A symbol-rate one GROD, $\boldsymbol{G}$, has the following properties:

a) There is no zero entry in $\boldsymbol{G}$;
b) Different entries in the same row or in the same column involve different indeterminates, i.e., $g_{ji} \neq \pm g_{j'i'}$ if either $j = j'$ or $i = i'$ (but not both);
c) The width of $\boldsymbol{G}$ is no greater than the height of $\boldsymbol{G}$, i.e., $N \leq P$;
d) The indeterminate x_k occurs N times in $\boldsymbol{G}$ for all $k \in \{1, 2, \ldots, K\} \triangleq \mathcal{K}$.

The proof is given in Appendix A.

For the ease of presentation, we express the half symbol-rate GCOD code matrix, after taking the transpose operation, in the following form [30]:

$$\boldsymbol{G}_c^T = \sum_{k=1}^{K} \boldsymbol{U}_k x_k^{(R)} + j \sum_{k=1}^{K} \boldsymbol{V}_k x_k^{(I)}, \tag{5}$$

where $\boldsymbol{U}_k$ and $\boldsymbol{V}_k$ are the associated $N \times 2P$ complex transmit matrices for $x_k^{(R)}$ and $x_k^{(I)}$, respectively. For example, consider the position of the complex indeterminate x_1 in $\boldsymbol{G}_c^3$ in (4). It is easy to see that the corresponding $\boldsymbol{U}_1$ and $\boldsymbol{V}_1$ are given below:

$$\boldsymbol{U}_1 = \begin{bmatrix} 1 & 0 & 0 & 0 & 1 & 0 & 0 & 0 \\ 0 & 1 & 0 & 0 & 0 & 1 & 0 & 0 \\ 0 & 0 & 1 & 0 & 0 & 0 & 1 & 0 \end{bmatrix},$$

$$\boldsymbol{V}_1 = \begin{bmatrix} 1 & 0 & 0 & 0 & -1 & 0 & 0 & 0 \\ 0 & 1 & 0 & 0 & 0 & -1 & 0 & 0 \\ 0 & 0 & 1 & 0 & 0 & 0 & -1 & 0 \end{bmatrix}.$$

According to [30], $\boldsymbol{U}_k$ and $\boldsymbol{V}_k$ have the following properties:

$$\boldsymbol{U}_k\boldsymbol{U}_k^\dagger = 2\boldsymbol{I}_N,\ \boldsymbol{V}_k\boldsymbol{V}_k^\dagger = 2\boldsymbol{I}_N,\ \forall k \in \mathcal{K}, \tag{6}$$

$$\boldsymbol{U}_k\boldsymbol{U}_m^\dagger = -\boldsymbol{U}_m\boldsymbol{U}_k^\dagger,\ \boldsymbol{V}_k\boldsymbol{V}_m^\dagger = -\boldsymbol{V}_m\boldsymbol{V}_k^\dagger,\ k, m \in \mathcal{K}, k \neq m, \tag{7}$$

$$\boldsymbol{U}_k\boldsymbol{V}_m^\dagger = \boldsymbol{V}_m\boldsymbol{U}_k^\dagger,\ \forall k, m \in \mathcal{K}. \tag{8}$$

The construction rule of $\boldsymbol{G}_c$ in (3) dictates that the corresponding $\boldsymbol{U}_k$ and $\boldsymbol{V}_k$ have a common left half submatrix, denoted by $\boldsymbol{C}_k$, for all k. Furthermore, their right half matrices are opposite in sign. We can express them as $\boldsymbol{U}_k = \begin{bmatrix} \boldsymbol{C}_k & \boldsymbol{C}_k \end{bmatrix}$ and $\boldsymbol{V}_k = \begin{bmatrix} \boldsymbol{C}_k & -\boldsymbol{C}_k \end{bmatrix}$. We summarize the properties of $\boldsymbol{C}_k$ in the following lemma. Note that (a) follows from Definition 1, (b) from Lemma 1(b), (c) from Lemma 1(d), and (d) from (b), (c), and Lemma 1(c).

Lemma 2: The common left half submatrix of $\boldsymbol{U}_k$ and $\boldsymbol{V}_k$, denoted by $\boldsymbol{C}_k$, has the following properties:

a) Each entry of $\boldsymbol{C}_k$ belongs to $\{0, +1, -1\}$;
b) In the same column or in the same row, the number of nonzero entries is at most one;
c) The number of nonzero entries is equal to N;
d) Each row consists of exactly one nonzero entry.

IV. GCOD combined with Adaptive Amplify-and-Forward

We apply the half symbol-rate GCOD code to the parallel relay network, with each relay acts as an antenna. After receiving a block of P symbols from the source, each relay node reshuffles the symbols according to the GCOD code and uses AAF to forward them to the destination. We call this protocol DOSTBC-AAF. In the next three subsections, we will describe the implementations at the source node, the relay nodes, and the destination node, respectively, within two consecutive transmission blocks. Afterwards, we will analyze the received SNR at the destination.

A. Implementation at the source node

At source A, a transmission block of $2P$ symbol times is divided into two equal-length sub-blocks. Source A transmits symbol $X_A[k]$ at time instant $k \in \mathcal{P}_{\text{real}}$ during the first sub-block, and keeps silent during the second sub-block.

B. Implementation at the relay nodes

The relay nodes, with each acting as a single antenna, apply the OSTBC cooperately in a distributed manner. Recall that we assume the relay nodes operate in full-duplex mode. At each relay node, the received noisy symbols within the first

sub-block act as basic entries for constructing a column of GCOD. More specifically, each relay reshuffles the order of its received symbols according to the half symbol-rate GCOD rule followed by amplitude change. After the reshuffling, the symbols are transmitted in the next transmission block. There is one block delay because a relay needs to store one block of received symbols before it can construct a new block of symbols.

Based on the GCOD rule, the j-th transmitted symbol by relay i within the first sub-block is given by

$$X_i[j] = \varphi_{ij}\xi_i Y_i[t_{ij}] = \Big(\xi_i h_{Ai}\Big)\Big(\varphi_{ij} X_A[t_{ij}]\Big) + \varphi_{ij}\xi_i w_i[t_{ij}], \quad j \in \mathcal{P}_{\text{real}}, i \in \mathcal{N}, \tag{9}$$

where $\varphi_{ij} \in \{-1, 1\}$ represents the sign of the (j,i)-th entry in $\boldsymbol{G}_c$, $\xi_i \leq \sqrt{\frac{P_i}{|h_{Ai}|^2 P_A + \delta_w^2}} \triangleq \xi_i^{\max}$ represents amplitude change/amplifying factor whose value depends on the instantaneous link gain of its input channel[1], and $t_{ij} \in \mathcal{P}_{\text{real}}$ represents the reshuffled order, i.e., the time index of the received symbol within previous transmission block, whose value is equal to the subscript of the (j,i)-th entry in $\boldsymbol{G}_c$. For the second sub-block, according to (3), the j-th transmission at relay i is given by

$$X_i[j] = (X_i[j-P])^*, \ j \in \mathcal{P}_{\text{comp}}, i \in \mathcal{N}. \tag{10}$$

C. Implementation at the destination node

If we stack the $2P$ received symbols at destination B for one transmission block to form a $2P \times 1$ column vector, then (2) for one transmission block can be written in matrix form as

$$\boldsymbol{y}_B = \boldsymbol{X}^T \boldsymbol{h}_B + \boldsymbol{w}_B, \tag{11}$$

where column vectors $\boldsymbol{w}_B \triangleq (w_B[1], \ldots, w_B[2P])$ and $\boldsymbol{y}_B \triangleq (Y_B[1], \ldots, Y_B[2P])$, and $N \times 2P$ matrix $\boldsymbol{X} \triangleq \big[X_i[j]\big]_{N \times 2P}$ with i as the row index and j as the column index.

As (9) shows, each entry of $\boldsymbol{X}$ contains two components: The first component is the amplified useful signal, and the second is the amplified noise. Hence, we can view matrix $\boldsymbol{X}$ as the sum of two matrices: One, denoted as $\boldsymbol{X}_s$, has the useful signal components as its entries; and the other, denoted as $\boldsymbol{X}_n$, has the noise components be its entries. Based on (9) and (10), we can express $\boldsymbol{X}_s$ and $\boldsymbol{X}_n$ as

$$\boldsymbol{X}_s = \boldsymbol{D}_{\xi h} \boldsymbol{X}_A, \tag{12}$$

$$\boldsymbol{X}_n = \boldsymbol{D}_{\xi} \boldsymbol{W}_R, \tag{13}$$

where $\boldsymbol{D}_{\xi h} \triangleq \text{diag}\{\xi_1 h_{A1}, \ldots, \xi_N h_{AN}\}$, $\boldsymbol{D}_{\xi} \triangleq \text{diag}\{\xi_1, \ldots, \xi_N\}$, and definition of $\boldsymbol{X}_A$ and $\boldsymbol{W}_R$ can be seen in (14) and (15) at the top of next page. Note that each entry of the left half submatrix in $\boldsymbol{W}_R$ is defined as $\tilde{w}_i[j] \triangleq \varphi_{ij} w_i[j]$, $i \in \mathcal{N}$, $j \in \mathcal{P}_{\text{real}}$. Clearly, $\tilde{w}_i[j]$ follows the same distribution as $w_i[j]$. Based on the specification of value t_{ij} in previous subsection and Lemma 1(b), we can easily obtain that index t_{ij} of each entry in $\boldsymbol{W}_R$ has the following property:

[1]This means that the relay node adopts AAF, with the amplifying factor ξ_i subject to a constraint which is characterized by the average power constraint within a codeword. Note that our constraint on ξ_i is identical to that in (9) of [20].

Lemma 3: If $j_1 \neq j_2$, then $t_{ij_1} \neq t_{ij_2}$, $i \in \mathcal{N}, j_1, j_2 \in \mathcal{P}_{\text{real}}$.

Recall that $\boldsymbol{X}_A$ is formed according to the GCOD code matrix, and thus can be decomposed according to (5). After the decomposition, we substitute (12) and (13) into (11) to obtain

$$\boldsymbol{y}_B = \Bigg(\sum_{k=1}^{K} \boldsymbol{D}_{\xi h} \boldsymbol{U}_k X_A[k]^{(R)} + j \sum_{k=1}^{K} \boldsymbol{D}_{\xi h} \boldsymbol{V}_k X_A[k]^{(I)} + \boldsymbol{D}_{\xi} \boldsymbol{W}_R\Bigg)^T \boldsymbol{h}_B + \boldsymbol{w}_B, \tag{16}$$

$$= \sum_{k=1}^{K} \boldsymbol{U}_k^T \boldsymbol{h}_{eq} X_A[k]^{(R)} + j \sum_{k=1}^{K} \boldsymbol{V}_k^T \boldsymbol{h}_{eq} X_A[k]^{(I)} + \boldsymbol{W}_R^T \boldsymbol{D}_{\xi} \boldsymbol{h}_B + \boldsymbol{w}_B, \tag{17}$$

where $\boldsymbol{h}_{eq} \triangleq \boldsymbol{D}_{\xi h}^T \boldsymbol{h}_B = \boldsymbol{D}_{\xi h} \boldsymbol{h}_B = \text{diag}\{\xi_1 h_{A1} h_{1B}, \ldots, \xi_N h_{AN} h_{NB}\}$.

We use the decorrelator and the maximal ratio combiner (MRC) at the receiver. In particular, we decompose the detection problem for the P transmitted symbols within a transmission block into P parallel problems and uses MRC to combine the corresponding signals from the N relay nodes. The parallelization and the MRC can be simultaneously achieved by right multiplying the received symbol vector $\boldsymbol{y}_B$ by $\boldsymbol{h}_{eq}^{\dagger} \boldsymbol{U}_m^*$ for all $m \in \mathcal{P}_{\text{real}}$ so as to detect the real part, and $-j\boldsymbol{h}_{eq}^{\dagger} \boldsymbol{V}_m^*$ for all $m \in \mathcal{P}_{\text{real}}$ so as to detect the imaginary part.

We denote the estimated value of $X_A[m]$ by $\hat{X}_A[m]$ for $m \in \mathcal{K}$. Its real part and imaginary part are given by $\hat{X}_A[m]^{(R)} = \text{Re}\Big\{\text{tr}\big(\boldsymbol{y}_B \boldsymbol{h}_{eq}^{\dagger} \boldsymbol{U}_m^*\big)\Big\}$ and $\hat{X}_A[m]^{(I)} = \text{Im}\Big\{\text{tr}\big(\boldsymbol{y}_B \boldsymbol{h}_{eq}^{\dagger} \boldsymbol{V}_m^*\big)\Big\}$, respectively. Following (17), $\hat{X}_A[m]$ can be expressed as the sum of three terms:

$$\hat{X}_A[m] = x_{m,A} + w_{m,B} + w_{m,R}. \tag{18}$$

The last two terms arise from the noise signals at relays and at the destination, and are given by

$$w_{m,B} = \text{Re}\{\text{tr}(\boldsymbol{w}_B \boldsymbol{h}_{eq}^{\dagger} \boldsymbol{U}_m^*)\} + j\text{Im}\{\text{tr}(\boldsymbol{w}_B \boldsymbol{h}_{eq}^{\dagger} \boldsymbol{V}_m^*)\}, \tag{19}$$

and

$$w_{m,R} = \text{Re}\{\text{tr}(\boldsymbol{W}_R^T \boldsymbol{D}_{\xi} \boldsymbol{h}_B \boldsymbol{h}_{eq}^{\dagger} \boldsymbol{U}_m^*)\} + j\text{Im}\{\text{tr}(\boldsymbol{W}_R^T \boldsymbol{D}_{\xi} \boldsymbol{h}_B \boldsymbol{h}_{eq}^{\dagger} \boldsymbol{V}_m^*)\}, \tag{20}$$

respectively. The first term of (18) arises from the data symbol, whose real and imaginary parts are

$$x_{m,A}^{(R)} = \text{tr}\big(\boldsymbol{h}_{eq} \boldsymbol{h}_{eq}^{\dagger} \boldsymbol{U}_m^* \boldsymbol{U}_m^T\big) X_A[m]^{(R)} + \sum_{k=1, k\neq m}^{K} \text{Re}\Big\{\text{tr}\big(\boldsymbol{h}_{eq} \boldsymbol{h}_{eq}^{\dagger} \boldsymbol{U}_m^* \boldsymbol{U}_k^T\big)\Big\} X_A[m]^{(R)} + \sum_{k=1}^{K} \text{Re}\Big\{j\text{tr}\big(\boldsymbol{h}_{eq} \boldsymbol{h}_{eq}^{\dagger} \boldsymbol{U}_m^* \boldsymbol{V}_k^T\big)\Big\} X_A[m]^{(I)}, \tag{21}$$

$$\boldsymbol{X}_A \triangleq \begin{bmatrix} \varphi_{11}X_A[t_{11}] & \cdots & \varphi_{1P}X_A[t_{1P}] & \left(\varphi_{11}X_A[t_{11}]\right)^* & \cdots & \left(\varphi_{1P}X_A[t_{1P}]\right)^* \\ \vdots & \ddots & \vdots & \vdots & \ddots & \vdots \\ \varphi_{N1}X_A[t_{N1}] & \cdots & \varphi_{NP}X_A[t_{NP}] & \left(\varphi_{N1}X_A[t_{N1}]\right)^* & \cdots & \left(\varphi_{NP}X_A[t_{NP}]\right)^* \end{bmatrix}, \tag{14}$$

$$\boldsymbol{W}_R \triangleq \begin{bmatrix} \tilde{w}_1[t_{11}] & \cdots & \tilde{w}_1[t_{1P}] & \left(\tilde{w}_1[t_{11}]\right)^* & \cdots & \left(\tilde{w}_1[t_{1P}]\right)^* \\ \vdots & \ddots & \vdots & \vdots & \ddots & \vdots \\ \tilde{w}_N[t_{N1}] & \cdots & \tilde{w}_N[t_{NP}] & \left(\tilde{w}_N[t_{N1}]\right)^* & \cdots & \left(\tilde{w}_N[t_{NP}]\right)^* \end{bmatrix}. \tag{15}$$

and

$$\begin{aligned} x_{m,A}^{(I)} &= \mathrm{tr}\big(\boldsymbol{h}_{eq}\boldsymbol{h}_{eq}^{\dagger}\boldsymbol{V}_m^*\boldsymbol{V}_m^T\big)X_A[m]^{(I)} \\ &\quad + \sum_{k=1,k\neq m}^{K} \mathrm{Re}\Big\{\mathrm{tr}\big(\boldsymbol{h}_{eq}\boldsymbol{h}_{eq}^{\dagger}\boldsymbol{V}_m^*\boldsymbol{V}_k^T\big)\Big\}X_A[m]^{(I)} \\ &\quad + \sum_{k=1}^{K} \mathrm{Im}\Big\{\mathrm{tr}\big(\boldsymbol{h}_{eq}\boldsymbol{h}_{eq}^{\dagger}\boldsymbol{V}_m^*\boldsymbol{U}_k^T\big)\Big\}X_A[m]^{(R)}. \end{aligned} \tag{22}$$

According to (7) and (8), all the individual terms within the summations are equal to zero (see also [30]). Removing the zero terms and using (6), we obtain

$$\begin{aligned} \hat{X}_A[m] &= 2\mathrm{tr}(\boldsymbol{h}_{eq}\boldsymbol{h}_{eq}^{\dagger})X_A[m] + w_{m,B} + w_{m,R} \\ &= 2||\boldsymbol{h}_{eq}||_F^2 X_A[m] + w_{m,B} + w_{m,R}, \end{aligned} \tag{23}$$

where $||\boldsymbol{h}_{eq}||_F^2$ represents the squared Frobenius norm.

D. SNR Analysis

To derive the received SNR at destination, we need to derive the variance of $w_{m,B}$ and $w_{m,R}$. Based on (19) and (20), and the properties of $\boldsymbol{U}_m$ and $\boldsymbol{V}_m$, it is easy to verify that the real part and the imaginary part of $w_{m,B}$ are independent and follow Gaussian distribution with identical variance. This property is also possessed by $w_{m,R}$. Hence, both $w_{m,B}$ and $w_{m,R}$ are circular symmetric complex Gaussian random variables. According to [31], we can obtain that $w_{m,B} \sim \mathcal{CN}\big(0, 2||\boldsymbol{h}_{eq}||_F^2\delta_w^2\big)$. Furthermore, we have:

Lemma 4: $w_{m,R} \sim \mathcal{CN}\Big(0, 4\big\|\mathrm{Re}\big\{\boldsymbol{g}_{eq}\boldsymbol{h}_{B\xi}^T\big\}\big\|_F^2\delta_w^2\Big)$, where column vectors $\boldsymbol{g}_{eq} \triangleq \mathrm{diag}\{\xi_1 h_{A1}h_{1B}^*, \ldots, \xi_N h_{AN}h_{NB}^*\}$ and $\boldsymbol{h}_{B\xi} \triangleq (\xi_1 h_{1B}, \ldots, \xi_N h_{NB})$.

The proof can be found in Appendix B.

Note that the transmission power of the source node and the variances of $w_{m,B}$ and $w_{m,R}$ do not depend on m. We hence define Γ_B as the received SNR at node B for symbol $\hat{X}_A[m]$, for $m \in \mathcal{K}$.

Theorem 5: The received SNR at destination B by DOSTBC-AAF for each transmitted symbol is

$$\Gamma_B = \frac{4\big(||\boldsymbol{h}_{eq}||_F^2\big)^2}{4\big\|\mathrm{Re}\big\{\boldsymbol{g}_{eq}\boldsymbol{h}_{B\xi}^T\big\}\big\|_F^2 + 2||\boldsymbol{h}_{eq}||_F^2}\Gamma \tag{24}$$

$$\geq \frac{||\boldsymbol{h}_{eq}||_F^2}{||\boldsymbol{h}_{B\xi}||_F^2 + 1/2}\Gamma \triangleq \underline{\Gamma}_B. \tag{25}$$

Proof: Equation (24) follows directly from (23) and the variances of $w_{m,B}$ and $w_{m,R}$. Since $\mathrm{Re}\{z_1 z_2\} \leq |z_1||z_2|$ for arbitrary complex numbers z_1 and z_2, the left term in the denominator of (24) is upper bounded by $4\Big\|\big|\boldsymbol{g}_{eq}\big|_E\big|\boldsymbol{h}_{B\xi}^T\big|_E\big|\Big\|_F^2 = 4||\boldsymbol{h}_{eq}||_F^2||\boldsymbol{h}_{B\xi}||_F^2$, where $|\cdot|_E$ represents the element-wise magnitude operation. Then, cancelling the common term $||\boldsymbol{h}_{B\xi}||_F^2$ between the numerator and the denominator, we obtain (25). ■

V. Optimization by Power Control

The outage probability of DOSTBC-AAF is given by $p_{out} = \Pr\{\Gamma_B < \Gamma_{thd}\}$. Clearly, the outage probability depends on the amplifying factors used by the relay nodes. If all relay nodes transmit with full power (FP), we call the resulting strategy DOSTBC-AAF (FP), but it may not be a good option. In the following, we investigate how to minimize p_{out} by adjusting the amplifying factors.

Since it is difficult to minimize p_{out} directly, we minimize $p_{out}^{\mathrm{UBD}} = \Pr\{\underline{\Gamma}_B < \Gamma_{thd}\}$, which is an upper bound of p_{out}, instead. To solve this minimization problem, we first note that the condition $\underline{\Gamma}_B < \Gamma_{thd}$ is equivalent to $f(\xi_1, \xi_2, \ldots, \xi_N) \triangleq \sum_{i=1}^{N}\xi_i^2|h_{iB}|^2\Gamma_i - \Gamma_{thd}\Big(\sum_{i=1}^{N}\xi_i^2|h_{iB}|^2 + \frac{1}{2}\Big) < 0$. Differentiating f with respect to ξ_i for all $i \in \mathcal{N}$, we obtain $\frac{\partial f}{\partial \xi_i} = 2\xi_i|h_{iB}|^2(\Gamma_i - \Gamma_{thd})$. It can be seen that f is a monotonic function of ξ_i. Whether it is increasing or decreasing depends on the sign of $\Gamma_i - \Gamma_{thd}$. Therefore, we have the following result:

Lemma 6: If $\Gamma_i < \Gamma_{thd}$ for all $i \in \mathcal{N}$, then $p_{out}^{\mathrm{UBD}} = 1$ for all ξ_i's, $i \in \mathcal{N}$.

Proof: Since f is monotonically decreasing with ξ_i for $i \in \mathcal{N}$, the global maximum of f occurs at $\xi_i = 0$ for all $i \in \mathcal{N}$. The statement follows from the fact that $f(0, 0, \ldots, 0) = -\frac{\Gamma_{thd}}{2} < 0$. ■

The above lemma indicates that it does not matter how we set the amplifying factors when all Γ_i's are less than the threshold. Now we consider the case where at least one of the received SNR's at the relay nodes are greater than the threshold. Denote the optimal amplifying factors that minimize p_{out}^{UBD} by ξ_i^*, $i \in \mathcal{N}$. The following result follows directly from the monotonicity of f:

Theorem 7: If not all Γ_i's are less than Γ_{thd}, then the minimizer of p_{out}^{UBD} satisfies the following conditions: For $i \in \mathcal{N}$,

$$\begin{cases} \text{if } \Gamma_i > \Gamma_{thd}, & \text{then } \xi_i^* = \xi_i^{\max}, \\ \text{if } \Gamma_i < \Gamma_{thd}, & \text{then } \xi_i^* = 0, \\ \text{if } \Gamma_i = \Gamma_{thd}, & \text{then } \xi_i^* \in [0, \xi_i^{\max}]. \end{cases}$$

Due to the randomly distributed nature of the link gains, the probability that $\xi_i^* \in (0, \xi_i^{\max})$ is zero. Therefore, ξ_i^* is either

zero or one, with probability one. We therefore call the above rule on-off power control (OOPC). When OOPC is applied to DOSTBC-AAF, we call the resulting strategy DOSTBC-AAF (OOPC). Though OOPC may not be optimal for DOSTBC-AAF, it does achieve diversity gain upon FP, which is verified numerically in Section VI. Note that DOSTBC-AAF (OOPC) can be implemented in a distributed way, since ξ_i^* of relay i does not depend on any information from the other relay nodes.

We then investigate the DMT [32], [33, Sec. 9.1.1] of DOSTBC-AAF (OOPC) in the high SNR regime, assuming that all the link gains follow i.i.d. Rayleigh fading. A diversity gain $d(r)$ is said to be achieved at multiplexing gain r if $R_\epsilon = r \log \Gamma$ and $\lim_{\Gamma\to\infty} \frac{\log_2 p_{out}(\Gamma)}{\log_2 \Gamma} = -d(r)$. Based on the proof in Appendix C, we have

Theorem 8: If all the link gains of the parallel relay network follow i.i.d. Rayleigh fading, DOSTBC-AAF (OOPC) achieves DMT $d(r) = N(1-2r),\ r \in [0, 0.5]$.

VI. Simulation Results

In this section, we examine our proposed schemes via computer simulations. Each point in the curves is obtained by Monte-Carlo simulations through averaging over 30 million channel realizations.

We first consider the diversity gain obtained by our system. The outage probability of DOSTBC-AAF (FP) and DOSTBC-AAF (OOPC) when the number of relay nodes, N, is equal to 4, 6, and 8, respectively, are plotted in Fig. 2. We assume that channel gains follow i.i.d. Rayleigh distribution with identical variance. In the simulation, we set $\kappa = 1$, $\Gamma_{thd} = 10$. We can see that the three curves obtained by DOSTBC-AAF (FP) with different values of N are parallel in the high SNR regime, which reveals that DOSTBC-AAF (FP) only achieves diversity order one no matter how many intermediate parallel relay nodes there are. That result agrees with the observation for Scheme 3 in [27]. Besides, it indicates that the use of multiple parallel relay nodes can only be used to reap power gain rather than diversity gain, which is not so effective. However, simulation result shows that if OOPC rule is adopted, the slope of the three curves changes with the choice of N, and the maximal diversity order of N can be achieved, which agrees with Theorem 8 for the special case where $r = 0$. This phenomenon can be explained intuitively as follows: When the link between the source and a certain relay node is weak, noise dominates useful signal at this relay node. Hence, the amplified noise is strong and will hamper the joint detection at the destination. Therefore, a good choice is to keep the relay off. Similarly, letting the relay transmit with full power is a good option if the link between source and this relay is good as the amplification of useful signal dominates the noise.

Next we investigate the DMT of DOSTBC-AAF with and without power control. We plot the DMT curves for DOSTBC-AAF (FP) and DOSTBC-AAF (OOPC) in Fig. 3. Note that the curve for the case with OOPC is obtained analytically, whereas that for the case with FP is only a conjecture. We have observed from Fig. 2 that FP can only yield diversity order of one, which verifies the point $(r, d) = (0, 1)$ in Fig. 3. For $N = 4$, we consider the cases where $r = 1/4$ and $r = 3/8$. We let $R_\epsilon = r \log_2 \Gamma$. In other words, we increase R_ϵ logarithmically with the SNR, and plot the corresponding outage probabilities of the two schemes against SNR in Fig. 4. It can be seen that for $r = 1/4$, the diversity orders of DOSTBC-AAF (OOPC) and DOSTBC-AAF (FP) are equal to 2 and 1/2, respectively, and for $r = 3/8$, they are equal to 1 and 1/4, respectively. These results agree with the analytical result for OOPC and the conjecture for FP. Other cases of the conjecture can also be verified by simulations.

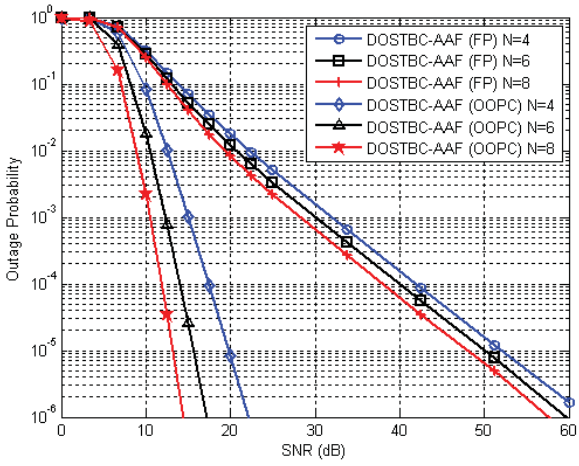

Fig. 2. Comparison of outage probability between DOSTBC-AAF (FP) and DOSTBC-AAF (OOPC).

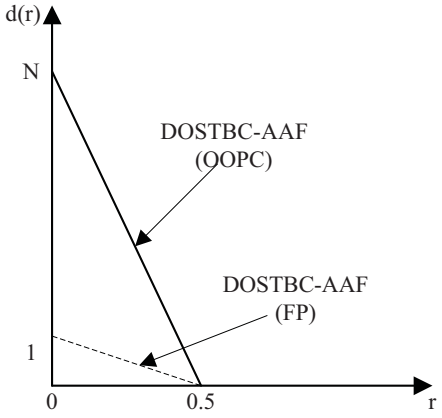

Fig. 3. Diversity-Multiplexing Tradeoff curves for DOSTBC-AAF (FP) and DOSTBC-AAF (OOPC) (The dashed curve is a conjecture based on simulation result).

VII. Conclusion

The outage performance of DOSTBC-AAF scheme for a two-hop parallel relay network is analyzed. Our numerical result shows that simply allowing the relay nodes transmit with FP fails to achieve the maximal diversity. Motivated by its poor performance, we derive an OOPC rule for DOSTBC-AAF. When this rule is applied, DOSTBC-AAF achieves the maximal diversity order. From DMT viewpoint, OOPC achieves significant improvement over FP for DOSTBC-AAF. More specifically, the achieved diversity order by OOPC is N

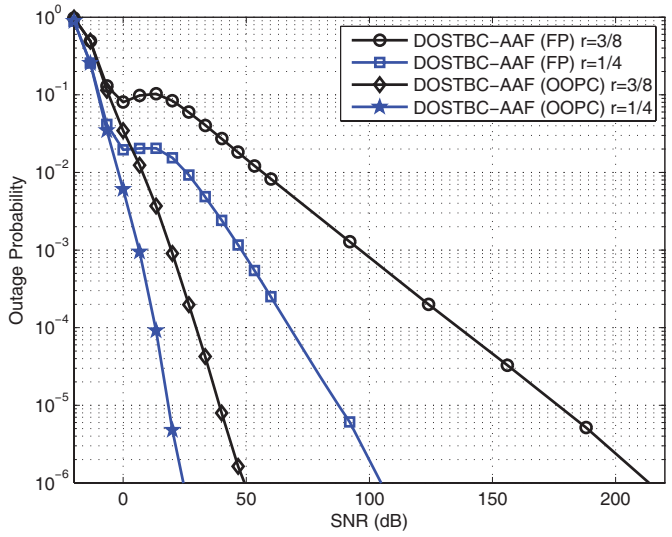

Fig. 4. Outage performance comparison of DOSTBC-AAF (FP) and DOSTBC-AAF (OOPC) for $N = 4$.

times of that by FP when their multiplexing gains are set to be identical.

Appendix A
Proof of Lemma 1

Proof: By definition, $\boldsymbol{G}$ satisfies $\boldsymbol{G}^T\boldsymbol{G} = \Big(\sum_{k=1}^{K} x_k^2\Big) I_N$. The norm of each column of $\boldsymbol{G}$ is thus the sum of K terms. Since the length of each column, P, is equal to K, no entry can be a zero. In addition, since each of the K terms in the sum involves distinct indeterminate, the entries in a column of $\boldsymbol{G}$ must also involve distinct indeterminates.

Next we consider the entries in the j-th row of $\boldsymbol{G}$. Suppose there exist g_{ji_1} and g_{ji_2} such that $g_{ji_1} = \pm g_{ji_2}$ for some $i_1 \neq i_2$. Denote the columns corresponding to the i_1-th and i_2-th as C_{i_1} and C_{i_2}, respectively. Due to the orthogonality of $\boldsymbol{G}$, we have $C_{i_1}^T C_{i_2} = 0$, which implies that there exists another row $j' \neq j$ such that $g_{j'i_1} = \pm g_{ji_1}$ and $g_{j'i_2} = \pm g_{ji_2}$, which contradicts with the fact that different entries in the same column of $\boldsymbol{G}$ involve different indeterminates.

Part (c) then follows from the fact that there are only K indetermines and the entries in each row must involve distinct indeterminates.

According to part (b), each indeterminate occurs once in each column. Part (d) follows from the fact that there are N columns. ∎

Appendix B
Proof of Lemma 4

Proof: We first consider the real part of $w_{m,R}$. Recall from (20) that $w_{m,R}^{(R)} = \mathrm{Re}\{\mathrm{tr}(\boldsymbol{W}_R^T \boldsymbol{D}_\xi \boldsymbol{h}_B \boldsymbol{h}_{eq}^\dagger \boldsymbol{U}_m^*)\} = \mathrm{Re}\{\mathrm{tr}(\boldsymbol{Z})\}$, where $\boldsymbol{Z} \triangleq \boldsymbol{U}_m^* \boldsymbol{W}_R^T \boldsymbol{D}_\xi \boldsymbol{h}_B \boldsymbol{h}_B^\dagger \boldsymbol{D}_{\xi h}$. The right part of $\boldsymbol{Z}$ is expressed as

$$\boldsymbol{D}_\xi \boldsymbol{h}_B \boldsymbol{h}_B^\dagger \boldsymbol{D}_{\xi h} = \begin{bmatrix} (\xi_1 h_{1B})(\xi_1 h_{A1} h_{1B}^*) & \cdots & (\xi_1 h_{1B})(\xi_N h_{AN} h_{NB}^*) \\ \vdots & \ddots & \vdots \\ (\xi_N h_{NB})(\xi_1 h_{A1} h_{1B}^*) & \cdots & (\xi_N h_{NB})(\xi_N h_{AN} h_{NB}^*) \end{bmatrix}. \tag{26}$$

We then calculate the left part, $\boldsymbol{U}_m^* \boldsymbol{W}_R^T$. We consider its transpose, $\boldsymbol{W}_R \boldsymbol{U}_m^\dagger$. Note that $\boldsymbol{W}_R$ is an $N \times 2P$ matrix, whereas $\boldsymbol{U}_m^\dagger$ is a $2P \times N$ matrix. Recall that $\boldsymbol{U}_m$ can be expressed in the form of $[\boldsymbol{C}_m \ \boldsymbol{C}_m]$, where $\boldsymbol{C}_m$ satisfies the properties in Lemma 2. According to Lemma 2(a) and (c), $\boldsymbol{C}_m$ has N non-zero entries, which may be either $+1$ or -1. Furthermore, by Lemma 2(d), each column of $\boldsymbol{C}_m^\dagger$ consists of exactly one non-zero entry. The i-th column of $\boldsymbol{W}_R \boldsymbol{U}_m^\dagger$ is thus obtained by adding two columns of $\boldsymbol{W}_R$, which are complex conjugate of each other, and then possibly followed by a sign change. Hence, we have

$$\boldsymbol{W}_R \boldsymbol{U}_m^\dagger = \begin{bmatrix} 2\phi_{11}\mathrm{Re}\{\tilde{w}_1[s_{11}]\} & \cdots & 2\phi_{1N}\mathrm{Re}\{\tilde{w}_1[s_{1N}]\} \\ \vdots & \ddots & \vdots \\ 2\phi_{N1}\mathrm{Re}\{\tilde{w}_N[s_{N1}]\} & \cdots & 2\phi_{NN}\mathrm{Re}\{\tilde{w}_N[s_{NN}]\} \end{bmatrix}, \tag{27}$$

where $\phi_{ij} \in \{+1, -1\}$ and s_{ij} takes the value of t_{pj} for certain $p \in \mathcal{P}_{\text{real}}$ for $i, j \in \mathcal{N}$. It is clear that $s_{ij} \in \mathcal{P}_{\text{real}}$ and it inherits the property of t_{ij} stated in Lemma 3, that is, if $j_1 \neq j_2$, then $s_{ij_1} \neq s_{ij_2}$.

Performing matrix multiplication on $\boldsymbol{U}_m^* \boldsymbol{W}_R^T$ and $\boldsymbol{D}_\xi \boldsymbol{h}_B \boldsymbol{h}_B^\dagger \boldsymbol{D}_{\xi h}$, then taking the trace, we obtain

$$\mathrm{tr}(\boldsymbol{Z}) = 2\sum_{j=1}^{N} \xi_j h_{Aj} h_{jB}^* \sum_{i=1}^{N} \xi_i h_{iB} \phi_{ij} \mathrm{Re}\{\tilde{w}_i[s_{ij}]\}. \tag{28}$$

Then, based on the above formula and the property of s_{ij}, we have

$$\mathrm{E}\Big[\big(w_{m,R}^{(R)}\big)^2\Big] = \mathrm{E}\Big[\Big(\mathrm{Re}\{\mathrm{tr}(\boldsymbol{Z})\}\Big)^2\Big] = \Big\|2\mathrm{Re}\Big\{\boldsymbol{g}_{eq}\boldsymbol{h}_{B\xi}^T\Big\}\Big\|_F^2 \frac{\delta_w^2}{2}. \tag{29}$$

Similarly, we can calculate the variance of the imaginary part as

$$\mathrm{E}\Big[\big(w_{m,R}^{(I)}\big)^2\Big] = 2\Big\|\mathrm{Re}\Big\{\boldsymbol{g}_{eq}\boldsymbol{h}_{B\xi}^T\Big\}\Big\|_F^2 \delta_w^2. \tag{30}$$

Summing up (29) with (30), we have the exact value of the variance. ∎

Appendix C
Proof of Theorem 8

The following lemma is needed:

Lemma 9: $\int_0^{+\infty} e^{-(u+\frac{c^2}{u})} du \geq e^{-2c}$.

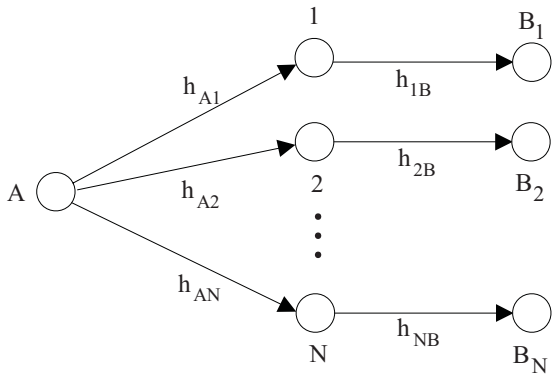

Fig. 5. Outage probability upper bound of DOSTBC-AAF (OOPC).

Proof: Setting $\theta \triangleq u + \frac{c^2}{u}$, we have $u = \frac{1}{2}\big(\theta \pm \sqrt{\theta^2 - 4c^2}\big)$. We then have

$$\begin{aligned}
&\int_0^{+\infty} e^{-(u+\frac{c^2}{u})} du \\
&= \int_c^{+\infty} e^{-(u+\frac{c^2}{u})} du + \int_0^{c} e^{-(u+\frac{c^2}{u})} du && (31)\\
&= \int_{2c}^{+\infty} e^{-\theta} d\Big(\frac{1}{2}\theta + \frac{1}{2}\sqrt{\theta^2 - 4c^2}\Big) \\
&\quad + \int_{+\infty}^{2c} e^{-\theta} d\Big(\frac{1}{2}\theta - \frac{1}{2}\sqrt{\theta^2 - 4c^2}\Big) && (32)\\
&= \frac{1}{2}\int_{2c}^{+\infty} e^{-\theta}\Big(1 + \frac{\theta}{\sqrt{\theta^2 - 4c^2}}\Big) d\theta \\
&\quad - \frac{1}{2}\int_{2c}^{+\infty} e^{-\theta}\Big(1 - \frac{\theta}{\sqrt{\theta^2 - 4c^2}}\Big) d\theta && (33)\\
&= \int_{2c}^{+\infty} e^{-\theta} \frac{\theta}{\sqrt{\theta^2 - 4c^2}} d\theta && (34)\\
&= \int_{2c}^{+\infty} e^{-\theta} d\sqrt{\theta^2 - 4c^2}. && (35)
\end{aligned}$$

Changing variables to $\varphi \triangleq \sqrt{\theta^2 - 4c^2}$, we have

$$\begin{aligned}
\int_0^{+\infty} e^{-(u+\frac{c^2}{u})} du &= \int_0^{+\infty} e^{-\sqrt{\varphi^2 + 4c^2}} d\varphi \\
&\geq \int_0^{+\infty} e^{-\sqrt{(\varphi + 2c)^2}} d\varphi \\
&= e^{-2c}. && (36)
\end{aligned}$$

■

Now we are ready to prove Theorem 8:

Proof: Since an exact diversity analysis for either p_{out} or p_{out}^{UBD} is very complicated, we consider another relaying model, whose outage probability is no less than p_{out}^{UBD}. This new model is obtained from the original model by splitting the destination, node B, into N virtual nodes, B_i for $i \in \mathcal{N}$, as shown in Fig. 5. There is no communication or cooperation among these virtual nodes so that joint decoding is impossible. The source and the relay nodes are assumed to operate in exactly the same way as in OOPC stated in Sec. IV and Sec. V. An outage occurs in the new system if all B_i's fail to decode the message, $i \in \mathcal{N}$.

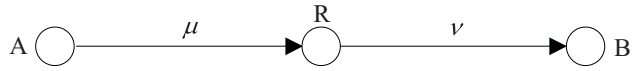

Fig. 6. Each subsystem.

In the new system, the received SNR's at destination B_i's satisfy the following conditions:

$$\begin{aligned}
\Gamma_{B_i} &= \frac{(\xi_i^{\max})^2 |h_{Ai}|^2 |h_{iB}|^2}{(\xi_i^{\max})^2 |h_{iB}|^2 + 1}\Gamma \\
&\leq \frac{(\xi_i^{\max})^2 |h_{Ai}|^2 |h_{iB}|^2}{(\xi_i^{\max})^2 |h_{iB}|^2 + 1/2}\Gamma \triangleq \overline{\Gamma}_{B_i},\ i \in \mathcal{N}_1 \triangleq \{i, \Gamma_i > \Gamma_{thd}\}, && (37)
\end{aligned}$$

$$\Gamma_{B_i} = 0 \triangleq \overline{\Gamma}_{B_i},\ i \in \mathcal{N}_2 \triangleq \{i, \Gamma_i < \Gamma_{thd}\}. \quad (38)$$

Recall that $\boldsymbol{\xi}^* = (\xi_1^*, \ldots, \xi_N^*)$ is the optimizer of $\underline{\Gamma}_B$. According to (25), (37) and (38), $\overline{\Gamma}_{B_i}$ is equal to $\underline{\Gamma}_B(\xi_i^* \boldsymbol{e}_i)$ if $i \in \mathcal{N}_1$, and $\underline{\Gamma}_B(\mathbf{0})$ if $i \in \mathcal{N}_2$, where $\boldsymbol{e}_i$ is the i-th standard basis and $\mathbf{0}$ is the zero vector. Therefore, $\underline{\Gamma}_B(\boldsymbol{\xi}^*) \geq \overline{\Gamma}_{B_i} \geq \Gamma_{B_i}$ for all $i \in \mathcal{N}$. Hence, the original model has a lower outage probability than the new one.

We then derive the DMT for the new system. Given a fixed spatial multiplexing gain, the diversity gain of the new system is N times of that achieved by each subsystem shown in Fig. 6. Within each subsystem, the source transmits during the first half time and keeps silent during the other half, the relay node adopts AAF with on-off power control, i.e., relay R uses maximal transmission power if $\Gamma_R > \Gamma_{thd}$ and keeps silent otherwise. It remains to prove that the DMT of each subsystem is $1 - 2r$.

In Fig. 6, μ and ν represent the square of the magnitude of the corresponding link gains, which experience independent Rayleigh fading. Therefore, they are independent exponential random variables, both with mean equal to one. Define $t \triangleq \frac{1}{\Gamma^{1-2r}}$ and $g(\mu, \nu) \triangleq \frac{\mu\nu}{\mu/\kappa + \nu + 1/(\kappa\Gamma)}$. Let ε be the event that an outage happens at relay R for spatial multiplexing gain r, i.e., $\log_2(1 + \Gamma_R) = \log_2(1 + \mu\Gamma) < 2r \log_2 \Gamma$, where the multiplicative factor 2 is due to the fact that the source transmits half of the time. The corresponding outage probability at relay R is $p_\varepsilon \triangleq \Pr\{\varepsilon\} \approx 1 - e^{-t}$.

If there is no outage in the first hop at relay R, relay R will transmit with full power and the achieved SNR at node B is $\Gamma_B = \frac{\mu\nu(\xi^{\max})^2}{\nu(\xi^{\max})^2 + 1}\Gamma = \frac{\mu\nu}{\mu/\kappa + \nu + 1/(\kappa\Gamma)}\Gamma = g(\mu, \nu)\Gamma$, where the definition of $\xi^{\max}$ for relay R is similar to that of ξ_i after (9). The corresponding outage probability at node B is

$$\begin{aligned}
q &\triangleq \Pr\{\log_2(1 + \Gamma_B) < 2r \log_2 \Gamma \mid \varepsilon^c\} && (39)\\
&\approx \Pr\{g(\mu, \nu) < t | \mu \geq t\} && (40)\\
&= \iint_{\mu \geq t, \frac{\mu\nu}{\mu/\kappa + \nu + 1/(\kappa\Gamma)} < t} e^{-\mu} e^{-\nu} d\mu d\nu && (41)\\
&= \int_t^{+\infty} e^{-\mu} d\mu \int_0^{\frac{\mu t/\kappa + t/(\kappa\Gamma)}{\mu - t}} e^{-\nu} d\nu && (42)\\
&= \int_t^{+\infty} e^{-\mu} d\mu \int_0^{\frac{\mu t/\kappa + t^2/(\kappa\Gamma^r)}{\mu - t}} e^{-\nu} d\nu && (43)\\
&= \int_t^{+\infty} e^{-\mu} d\mu - \int_t^{+\infty} e^{-\mu} e^{-\frac{\mu t/\kappa + t^2/(\kappa\Gamma^r)}{\mu - t}} d\mu. && (44)
\end{aligned}$$

Changing variables to $u \triangleq \mu - t$ and defining $d \triangleq \sqrt{(1+1/\Gamma^r)/\kappa}$, we have

$$q \approx e^{-t} - e^{-(1+1/\kappa)t} \int_0^{+\infty} e^{-u} e^{-\frac{t^2/\kappa + t^2/(\kappa\Gamma^r)}{u}} du$$
$$= e^{-t} - e^{-(1+1/\kappa)t} \int_0^{+\infty} e^{-(u+\frac{d^2t^2}{u})} du. \quad (45)$$

Based on Lemma 9, we have $q \leq e^{-t} - e^{-(1+1/\kappa)t} e^{-2dt}$. Hence, the outage probability of each sybsystem is upper bounded by $p_\varepsilon + (1-p_\varepsilon)q = (1+2d+1/\kappa)t + o(t) \leq \frac{(\frac{1+2\sqrt{2}}{\sqrt{\kappa}} + \frac{1}{\kappa})}{\Gamma^{1-2r}} + o(\frac{1}{\Gamma^{1-2r}})$. We then obtain that the DMT of each subsystem has the following lower bound: $d^{\text{subsys}}(r) \geq 1-2r,\ r \in [0, 0.5]$. Since the optimal DMT for the first hop is exactly the right hand side of the above inequality, strict inequality cannot hold, and the proof is completed. ■

REFERENCES

[1] T. L. Marzetta and B. M. Hochwald, "Capacity of a mobile multiple antenna communication link in Rayleigh flat fading," *IEEE Trans. Inf. Theory*, vol. 45, no. 1, pp. 139-157, May 1999.

[2] V. Tarohk, N. Seshadri, and A. R. Calderbank, "Space-time codes for high data rate wireless coomunication: performance analysis and code construction," *IEEE Trans. Inf. Theory*, vol. 44, no. 2, pp. 744-765, Mar. 1998.

[3] S. Alamouti, "A simple transmit diversity technique for wireless communications," *IEEE J. Sel. Areas Commun.*, vol. 16, no. 8, pp. 1451-1458, Oct. 1998.

[4] N. D. Sidiropoulos and R. S. Budampati, "Khatri-Rao space-time codes," *IEEE Trans. Signal Process*, vol. 50, no. 10, pp. 2396-2407, Oct. 2002.

[5] V. Tarokh, H. Jafarkhani, and A. R. Calderbank, "Space-time block codes from orthogonal designs," *IEEE Trans. Inf. Theory*, vol. 45, no. 5, pp. 1456-1467, July 1999.

[6] H. Jafarkhani, "A quasi-orthogonal space-time block code," *IEEE Trans. Commun.*, vol. 49, no. 1, pp. 1-4, Jan. 2001.

[7] W. Su and X.-G. Xia, "Signal constellations for quasi-orthogonal space-time block codes with full diversity," *IEEE Trans. Inf. Theory*, vol. 50, no. 10, pp. 2331-2347, Oct. 2004.

[8] B. Hassibi and B. M. Hochwald, "High-rate codes that are linear in space and time," *IEEE Trans. Inf. Theory*, vol. 44, no. 2, pp. 1804-1824, July 2002.

[9] M. O. Damen, K. Abed-Merim, and J. C. Belfiore, "Diagonal algebraic space-time block codes," *IEEE Trans. Inf. Theory*, vol. 48, no. 3, pp. 628-635, Mar. 2002.

[10] D. N. Dao, C. Tellambura, C. Yuen, T. T. Tjhung, and Y. L. Guan, "Four-group decodable semi-orthogonal algebraic space-time block codes," *Wireless Communications and Networking Conference*, Mar. 2007.

[11] D. N. Dao and C. Tellambura, "Capacity-approaching semi-orthogonal space-time block codes," in *Proc. IEEE GLOBECOM*, pp. 3305-3309, Nov. 2005.

[12] W. Su, "Orthogonal space-time block codes for wireless communications," Ph.D. dissertation, Univ. Delaware, Aug. 2002.

[13] W. Su and X.-G. Xia, "On space-time block codes from complex orthogonal designs," *Wireless Personal Commun.*, vol. 25, no. 1, pp. 1-26, Apr. 2003.

[14] H. Jafarkhani, "A quasi-orthogonal space-time block code," *IEEE Trans. Commun.*, vol. 49, no. 1, pp. 1-4, Jan. 2001.

[15] X.-B. Liang, "Orthogonal designs with maximal rates," *IEEE Trans. Inf. Theory*, vol. 49, no. 10, pp. 2468-2503, Oct. 2003.

[16] S. Borade, L. Zheng, and R. Gallager, "Amplify-and-forward in wireless relay networks: rate, diversity, and network size," *IEEE Trans. Inf. Theory*, vol. 53, no. 10, pp. 3302-3318, Oct. 2007.

[17] B. Schein and R. Gallager, "The Gaussian parallel relay network," in *Proc. International Symposium on Information Theory*, pp. 22, June 2000.

[18] F. Xue and S. Sandhu, "Cooperation in a half-duplex Gaussian diamond relay channel," *IEEE Trans. Inf. Theory*, vol. 53, no. 10, pp. 3806-3814, Oct. 2007.

[19] M. Kobayashi and X. Mestre, "Impact of CSI on distributed space-time coding in wireless relay networks," *IEEE Trans. Wireless Commun.*, vol. 8, no. 5, pp. 2580-2591, May 2009.

[20] J. N. Laneman, D. N. C. Tse, and G. W. Wornell, "Cooperative diversity in wirelss networks: efficient protocols and outage behavior," *IEEE Trans. Inf. Theory*, vol. 50, no. 12, pp. 3062-3080, Dec. 2004.

[21] J. N. Laneman and G. W. Wornell, "Distributed space-time-coded protocols for exploiting cooperative diversity in wireless networks," *IEEE Trans. Inf. Theory*, vol. 49, no. 10, pp. 2415-2425, Oct. 2003.

[22] R. Nabar, H. Bolcskei, and F. W. Kneubohler, "Fading relay channels: performance limits and space-time signal design," *IEEE J. Sel. Areas Commun.*, vol. 22, no. 6, pp. 1099-1109, Aug. 2004.

[23] Y. Hua, Y. Mei, and Y. Chang, "Parallel wireless mobile relays with space time modulations," in *Proc. IEEE Workshop on Statistical Signal Processing*, pp. 375-378, Sep. 2003.

[24] Y. Jing and B. Hassibi, "Distributed space-time coding in wireless relay networks," *IEEE Trans. Wireless Commun.*, vol. 5, no. 12, pp. 3524-3536, Dec. 2006.

[25] Z. Yi and I.-M. Kim, "Single-symbol ML decodable distributed STBCs for cooperative networks," *IEEE Trans. Inf. Theory*, vol. 53, no. 8, pp. 2977-2985, Aug. 2007.

[26] B. Maham and A. Hjϕrungnes, "Opportunistic relaying through amplify-and-forward distributed space-time codes with partial statistical CSI at relays," in *Proc. 46th Annual Allerton Conference on Commun., Control, and Computing*, pp. 1004-1008, Sep. 2008.

[27] B. Maham, A. Hjϕrungnes, and G. Abreu, "Distributed GABBA space-time codes in amplify-and-forward relay networks," *IEEE Trans. Wireless Commun.*, vol. 8, no. 4, pp. 2036-2045, Apr. 2009.

[28] M. Dai, P. Hu, and C. W. Sung "Diamond relay network under Rayleigh fading: on-off power control and outage-capacity bound," in *Proc. IEEE ISITA 2010*, Oct. 2010.

[29] X.-B. Liang and X.-G. Xia, "On the nonexistence of rate-one generalized complex orthogonal designs," *IEEE Trans. Inf. Theory*, vol. 49, no. 11, pp. 2984-2989, Nov. 2003.

[30] G. Ganesan and P. Stoica, "Space-time block codes: a maximum SNR approach," *IEEE Trans. Inf. Theory*, vol. 47, no. 4, pp. 1650-1656, May 2001.

[31] S. Sandhu and A. Paulraj, "Space-time block codes: a capacity perspective," *IEEE Commun. Lett.*, vol. 4, no. 12, pp. 384-386, Dec. 2000.

[32] L. Zheng and D. N. C. Tse, "Diversity and multiplexing: a fundamental tradeoff in multiple-antenna channels," *IEEE Trans. Inf. Theory*, vol. 49, no. 5, pp. 1073-1096, May 2003.

[33] D. Tse and P. Viswanath, *Fundamentals of Wireless Communication*. Cambridge University Press, 2004.

Mingjun Dai received the B.Eng and M.Phil degrees in control theory and engineering from the Harbin Institute of Technology, Harbin, China, in 2004 and 2006, respectively. He is currently a PhD candidate in the Department of Electronic Engineering at City University of Hong Kong. His research interests include cooperative relay network, and optimization of wireless networks.

Chi Wan Sung (M'98) received the B.Eng, M.Phil, and Ph.D. degrees in information engineering from the Chinese University of Hong Kong in 1993, 1995, and 1998, respectively. Afterwards, he became an Assistant Professor in the same university. He joined the faculty at City University of Hong Kong in 2000, and is now an Associate Professor with the Department of Electronic Engineering. His research interests include multiuser information theory, design and analysis of algorithms, and optimization of wireless networks.

Yan Wang received the B.Eng and M.Phil degrees in physical optics from the Harbin Institute of Technology, Harbin, China, in 2003 and 2005, respectively. Afterwards, he became an Telecommunication and Software Engineerer in ZTE Corp. His research interests include cooperative relay network, and CDMA system.